A simulation of the quasi 2-day wave and its effect on variability of the summertime mesopause temperature

D. Pendlebury, University of Toronto, Canada (diane@atmosp.physics.utoronto.ca)

Abstract

The quasi 2-day wave (Q2DW) is studied using a 20-year run of the Canadian Middle Atmosphere Model. The simulated Q2DW maximizes in amplitude shortly after solstice in the summer hemisphere. Unlike other studies, the wave exhibits a variable phase speed over each summer season, which decreases as the mesospheric jet decays. The period is intially shorter than 2 days, but lengthens to more than 2 days in some years. A 2-day wave index is derived, and is used to examine the effect of the 2-day wave on mesospheric temperatures through its impact on the residual circulation. Up to 10% of the interannual variability in the polar summer mesopause temperatures can be attributed to the simulated Q2DW, with temperature differences of up to 3-5 K.

Motivation

The quasi 2-day wave (Q2DW) is a persistent feature of the mesosphere. It has a period of approximately 2 days, and is dominated by zonal wavenumber 3. Its amplitude is largest shortly after solstice in the summer hemisphere, when it undergoes rapid growth due to baroclinic instability of the summer mesospheric jet. The region of baroclinic instability is formed by a torque that is generated by gravity waves that propagate from the troposphere to the mesosphere.

The same GWD is also responsible for producing a pole-to-pole circulation characterized by upwelling over the summer pole, downwelling over the winter pole, and a summer-to-winter circulation across the equator. This residual circulation can be affected by the presence of the Q2DW (Lieberman 1999).

The resulting adiabatic cooling that takes place over the summer pole is responsible for making the summer polar mesopause the coldest place on Earth. The extreme temperatures in this region allow for the formation of polar mesospheric clouds (PMCs). Their growth rate is highly sensitive to temperature, and their appearance is therefore an excellent indicator of small changes in the polar summer mesosphere (e.g. Lübken et al., 2009).

Photo: Polar mesospheric clouds over Kuresoo bog, Soomaa National Park, Estonia. Martin Koitmäe

The focus of this paper is two-fold: first, to examine the Q2DW as simulated by the extended version of the CMAM, and second, to study the effect of the wave on summer mesopause temperatures.

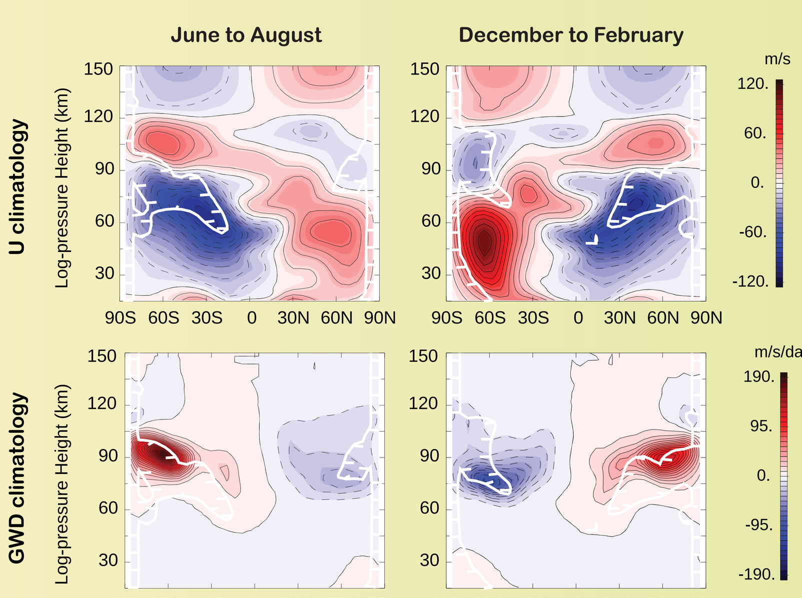

Figure 1: Climatology for NH summer (left column) and SH summer (right column) for zonal wind (top panels; contour interval of 10 m/s), and gravity wave drag in the zonal momentum budget (bottom panels; contour interval 10 m/s/day). The thick white line delineates the area where the meridional gradient of PV is negative.

Model and Methods

The upward extension of the Canadian Middle Atmosphere Model (CMAM) (McLandress et al., 2006) is used. It has a horizontal resolution of T32, and 95 vertical levels extending up to ~250 km. The climatologies for the zonal-mean zonal wind, and the zonal component of the GWD are shown in **Figure 1** for July to August (JJA, left column) and December to February (DJF, right column).

The summertime jets for JJA and DJF are comparable in magnitude between the hemispheres. As a result, the GWD in the summer hemisphere is similar. The GWD is responsible for the deceleration at the top of the summer jet and the wind reversal above, and gives rise to the region of negative meridional gradient of potential vorticity. Regions of negative Ertel's potential vorticity (PV) gradient ($1/a\ \partial P/\partial\varphi < 0$) are outlined by the thick white lines in **Figure 1**.

The Q2DW in the CMAM data is isolated by using a Fourier transform in longitude to isolate the zonal wavenumber 3 component. The amplitude of the Q2DW changes over time. In order to capture this behaviour, the S-transform (Stockwell et al., 1996) is used.

The analysis was performed for SH summer (December to March; DJFM) and NH summer (June to September; JJAS). The data is sampled every 6 hours. The focus will be on year 12 for JJAS, which provides a fairly typical example of the Q2DW during NH summer, and on year 09 for DJFM, which exhibits one of the largest and most persistent Q2DWs during SH summer.

The Quasi-2-Day Wave (Q2DW)

A snapshot of the amplitude and phase of the Q2DW (zonal wavenumber 3, 1.69 day period) in the meridional wind is shown in **Figure 2**. A period of 1.69 days was chosen since it is close to the maximum amplitude for both times shown. Regions of negative meridional gradient of PV, and the critical line for a wave with zonal wavenumber 3 and 1.69 day period. The critical line approximately follows the boundary of the region of negative PV gradient below 75-80 km.

Figure 3 shows the Q2DW amplitude in the meridional velocity at 88 km for 5 years of the simulation. Generally, the Q2DW is larger in amplitude and more persistent during NH summer, reaching amplitudes in excess of 50 m/s in v and 11 K in T, compared with the SH summer, during which the Q2DW reaches only 36 m/s in v and 8 K in T for the strongest years.

The Q2DW in the extended CMAM appears to be in good agreement with respect to several characteristics of the observed Q2DW; the seasonality of the amplification of the wave is approximately correct, and the amplitude in the SH summer is in agreement with the Q2DW derived from MLS temperatures and winds (Limpasuvan et al., 2005). In other aspects, the Q2DW is not so realistic; the maximum amplitude in the NH summer is in general too large, and the wave is too persistent with too little interannual variability.

The period of the Q2DW also changes over the course of the season, shown in **Figure 4** for year 12 of JJAS and year 09 of DJFM at a single location (47°N/S, 88 km). The wave forms early in the season with a period as short as ~1.5 days. Later in the season, the period lengthens to closer to 2 days. The phase speed of the wave approximately follows the zonal-mean zonal wind at the location where the PV gradient changes sign on the equatorward side of the jet between 60 and 75 km. Overlaid on **Figure 4** is the location in time-period space of the climatological average of the maximum amplitude at 88 km and 47°N/S (thick white line).

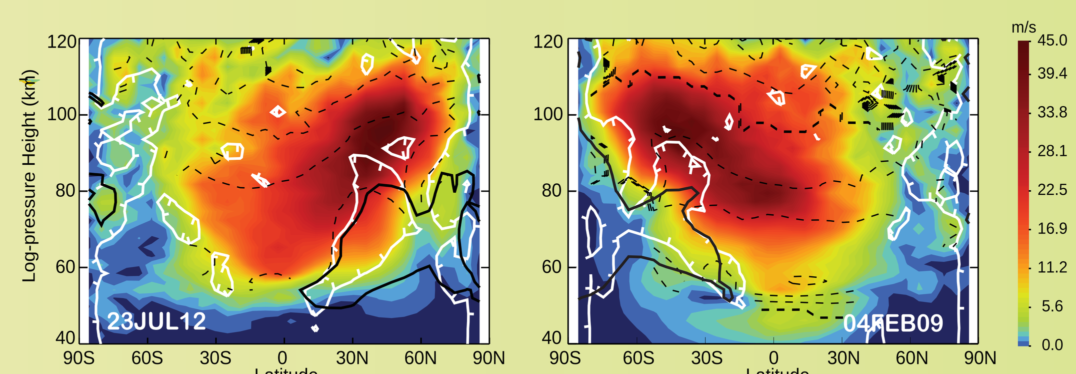

Figure 2: Amplitude of the Q2DW (zonal wavenumber 3 and 1.69 day period) in v for NH summer (left) and SH summer (right). Phase lines (dashed) are plotted every $\pi/4$ where the amplitude is above 5 m/s. The thick white line delineates the region of negative PV gradient, and the thick solid black line denotes the critical line for the wave.

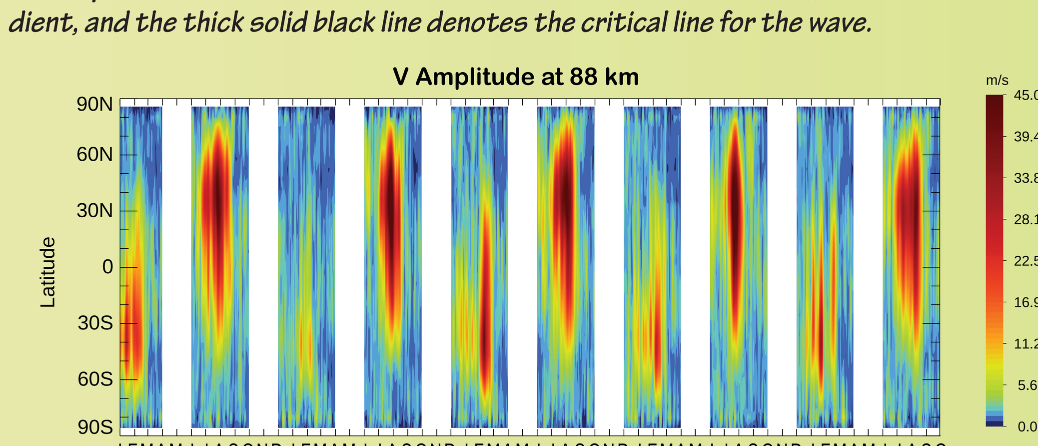

Figure 3: Interannual variability of the amplitude of the Q2DW in v at 88 km.

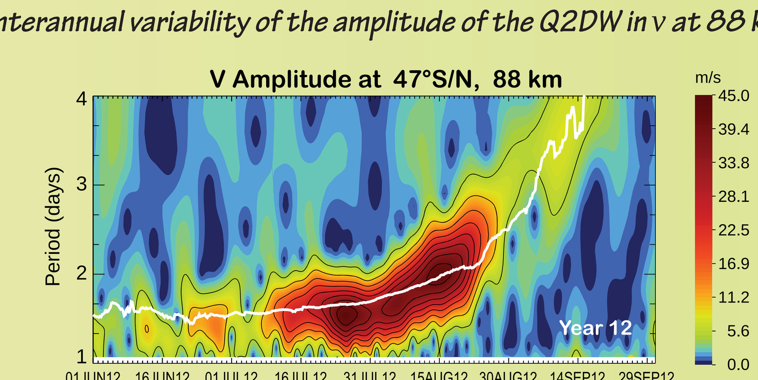

Figure 4: The wavenumber 3 amplitude in period versus time for NH summer year 12 at 47°N and 88 km. Contour interval is 5 m/s. The thick white line denotes the maximum amplitude in time-period space at this location averaged over 20 years.

Definition of the 2-day wave index

In order to study the effect of the Q2DW on the zonal mean state of the mesosphere, a "2-day wave" index is defined using Empirical Orthogonal Functions (EOFs) to represent the amplitude of the Q2DW in v. The EOF analysis is focused from 3°S/N to 80°S/N and from 70 km to 125 km.

Figure 5 shows the first two EOFs and their corresponding principal components (PCs) for each year. The first EOF explains 90% of the variance for the 2-day wave in the NH summer, and 80% of the variance in the SH summer. The spatial structure of the first EOF approximates the amplitude in v.

The Q2DW index I_{2dw} is defined as the principal component (PC) of the first EOF, such that I_{2dw} is always positive. Comparing I_{2dw} to the amplitude of the Q2DW, it is possible to see the corresponding variation between years. The Q2DW during NH summer is more persistent and shows less interannual variability, generally reaching a value of ~3-4. During SH summer, the Q2DW shows much more variability. I_{2dw} of the NH summer and that of the SH summer as defined here must be considered separately because the EOFs are calculated independently; a value of 4 in the NH summer is not equivalent to a value of 4 in the SH summer.

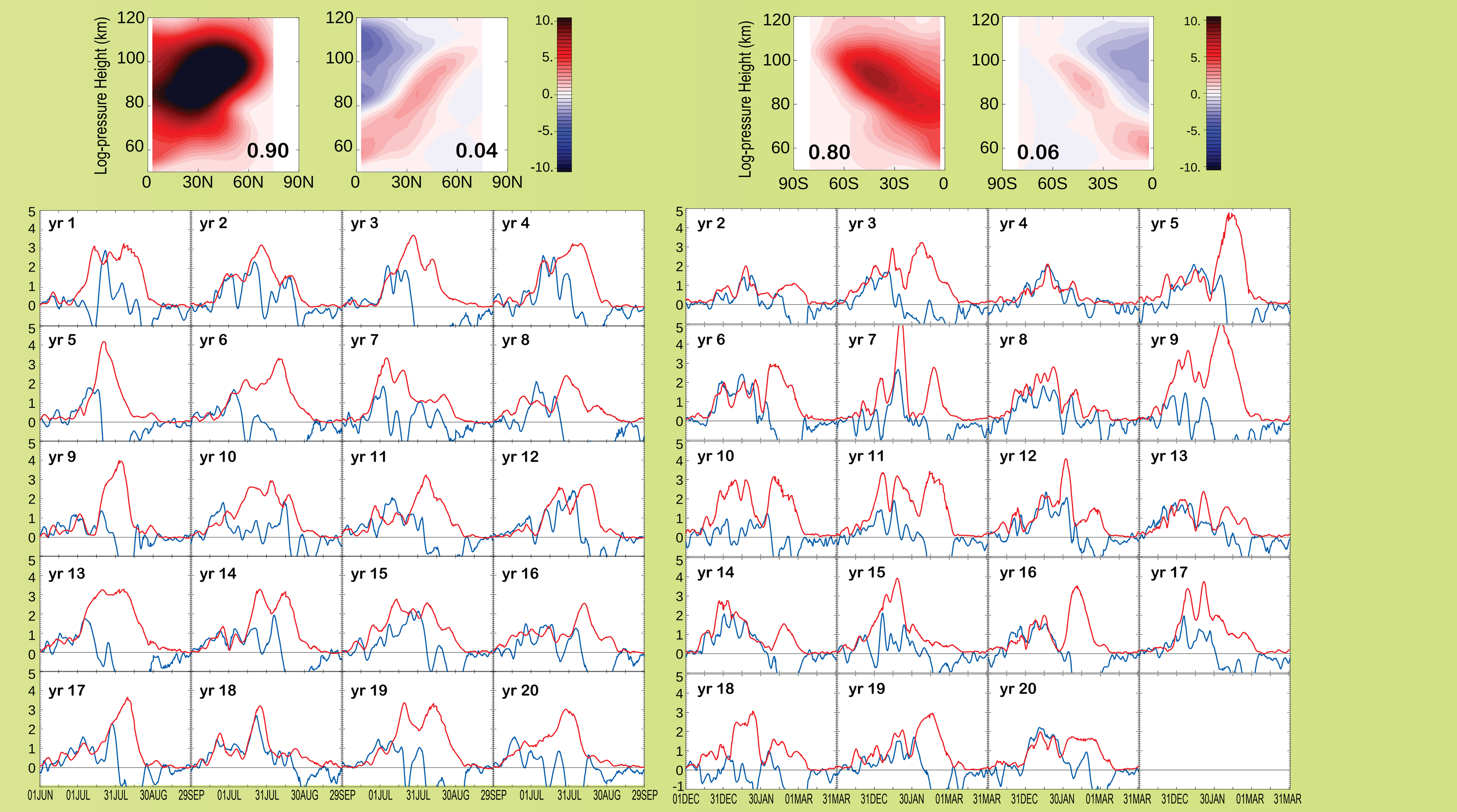

Figure 5: Above: The first and second EOFs of Q2DW amplitude in the meridional wind for JJAS (left) and DJFM (right). Below: The principal components (PCs) of the first (solid) and second (dashed) EOFs for each year. Values of 1.046 and 1.028 have been added to the PC for the first EOF so that they are always positive.

Effect of Q2DW on polar temperatures

The Q2DW can induce its own residual circulation, defined as

$$\bar{v}^*_{2dw} = -\frac{1}{\rho_o}\frac{\partial}{\partial z}\left(\rho_o\frac{\overline{v'\theta'}}{\theta_{0z}}\right)$$

where $(\bullet)'$ indicates the wave with zonal wavenumber 3 and period following the mean maximum amplitude. The $\bar{v}^*_{2dw}$ is shown in **Figure 6** by the coloured shading for year 12 of JJA and year 09 of DJF. The residual circulation induced by the Q2DW counteracts that driven by the GWD. The induced circulation of the Q2DW is quite weak in SH summer, whereas in the NH summer it appears to be almost the same magnitude as $\bar{v}^*$ itself. This difference is largely the result of the persistence of the Q2DW during NH summer.

To examine the possible impact of the Q2DW on summer polar mesopause temperatures, the temperature anomaly at the mesopause is averaged over 85-97 km and ~75° to the pole and averaged over the season. The strength of the Q2DW for each summer is determined by integrating I_{2dw} over the season. **Figure 7** shows the relationship between the temperature anomaly and the strength of the Q2DW.

The temperature anomaly at the summer polar mesopause is also controlled by the GWD anomaly. An EOF analysis was performed on the GWD. In this case, the first 3 EOFs were retained. During JJAS, the first three components explain 35.4%, 24.7% and 12.2% of the variance, and during DJFM, they explain 42.7%, 32.6% and 10.9% of the variance. The EOFs correspond to a strengthening/weakening of the climatological GWD (first EOF), a shift in altitude (second EOF) and a shift in latitude (third EOF). Years with larger GWD anomalies have colder summer mesopause temperatures (not shown).

To examine the temporal relationship between the Q2DW and summer polar mesopause temperature anomaly, multiple linear regression (MLR) analysis is used. The model used for the temperature anomaly over the pole is:

$$\delta T(t) = A_0 + A_{2dw}I_{2dw}(t) + A_{GW1}P_{GW1}(t) + A_{GW2}P_{GW2}(t) + A_{GW3}P_{GW3}(t) + \varepsilon$$

where A are the MLR coefficients, P_{GWi} is the principal component of the i^{th} EOF of the GWD anomaly, and ε is the residual. In order to ensure that the residuals are Gaussian and have no auto-correlation, 5-day averages were used. **Figure 8** shows a sample period of the MLR analysis for NH summer. The largest component to the fit in δT is the first EOF for the GWD anomaly. However, when the Q2DW is active, it contributes significantly to the fit.

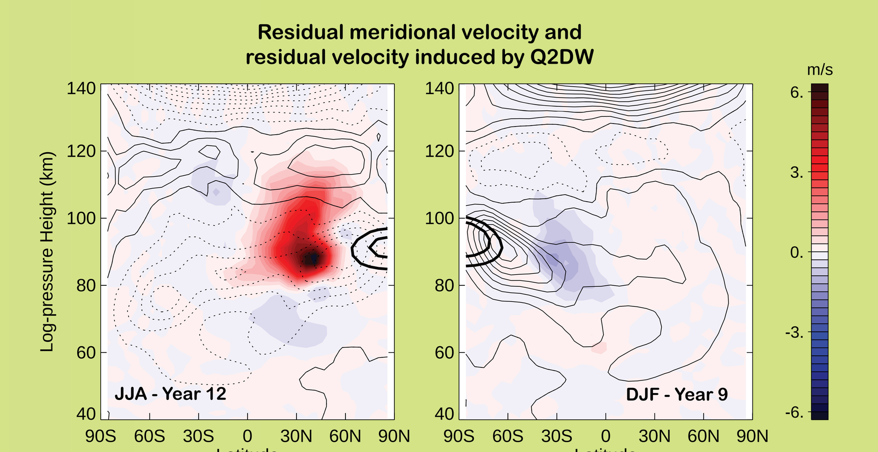

Figure 6: Climatological $\bar{v}^*$ for JJA (left panel) and DJF (right panel). Contour level is 2 m/s; solid (dashed) lines denote positive (negative) values. Colour shows $\bar{v}^*_{2dw}$ averaged over JJA for year 12 and DJF for year 09. The summer polar mesopause is shown by the thick black lines and indicate where the temperature climatology is less than 110 K and 130 K.

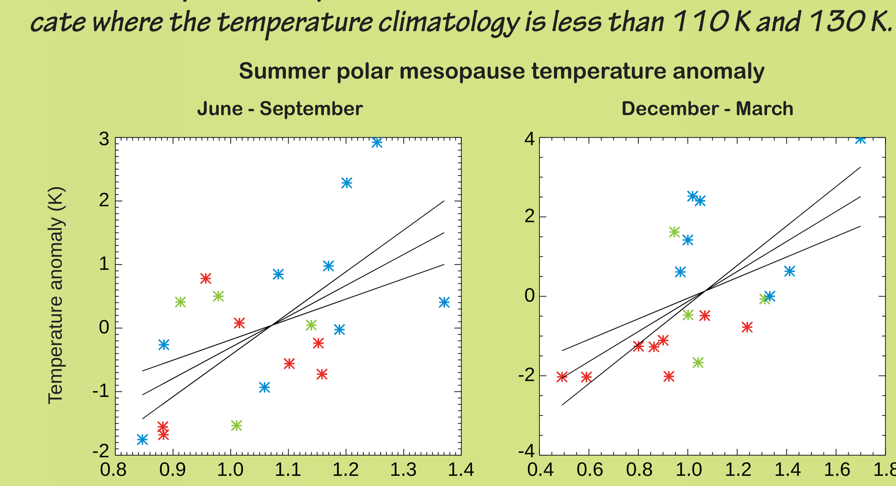

Figure 7: δT over the North Pole during JJAS (left) and over the South Pole during DJFM (right) versus the strength of the Q2DW. Colours indicate the strength of the GWD anomaly (blues are weaker years, greens are average and reds are stronger years). A linear fit to the data with 1σ uncertainty in the coefficients is shown.

Figure 9 shows the percent of the variance in the MLR fit explained by the Q2DW component (i.e., $\int A_{2dw}I_{2dw}(t)dt / \int \delta T(t)dt$) for each year versus the strength of the Q2DW. There is a clear correlation between the amount of variance explained and the strength of the Q2DW.

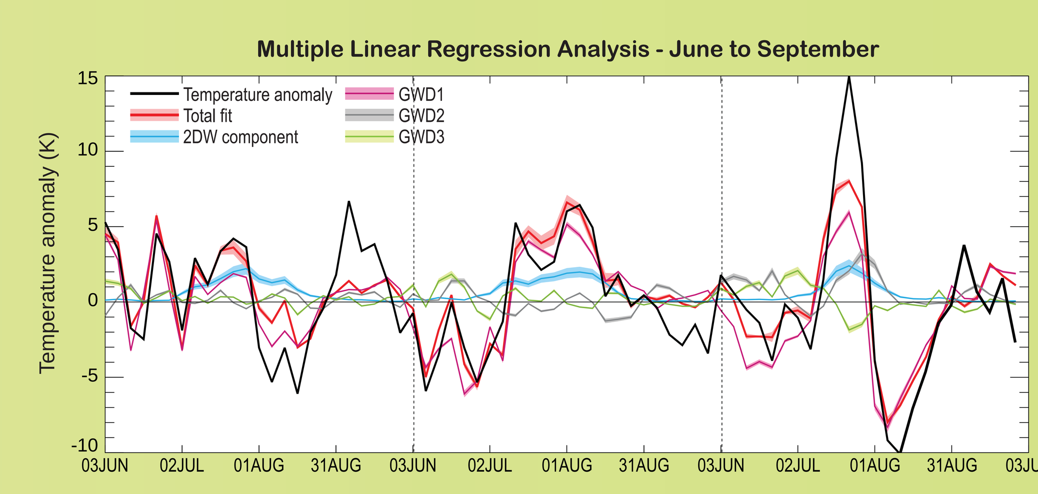

Figure 8: Actual temperature anomaly (5-day averages) and the MLR fit for June to September, years 02 to 04. Shading indicates the 1σ error of the MLR coefficients.

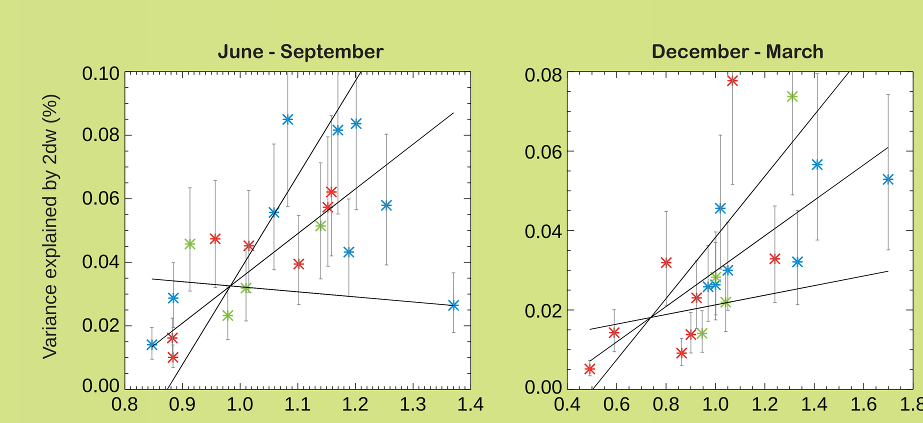

Figure 9: Variance explained by the Q2DW term in the MLR analysis on δT versus the strength of the Q2DW for JJAS (left) and DJFM (right). Error bars indicate the 1σ error in the fit to the MLR analysis. A linear fit to the data with the 1σ uncertainty in the linear fit coefficients is shown.

Concluding Remarks

An interesting feature of the simulated Q2DW is the lengthening of the period as the summer season progresses. This behaviour is due to the weakening of the mesospheric jet, and the adjustment of the critical line to the location of the boundary of the region of negative PV gradient. The period of the wave is highly sensitive to the background winds.

Using the 2-day wave index, there is a significant correlation with summer polar mesopause temperatures and the Q2DW; a strong Q2DW produces a warmer mesopause by up to 3-5 K. MLR analysis shows that the Q2DW can explain up to 10% of the seasonally averaged temperature anomaly at the mesopause.

McCormack et al. (2009) found that the 2006 SH summer Q2DW in the NOGAPS-ALPHA model was influenced by a stratospheric sudden warming in the winter hemisphere, through planetary waves impinging on a region of inertial instability on the summer side of the equator. This suggests that there may be a link between planetary wave activity in the winter hemisphere and the presence of the Q2DW in the summer hemisphere, and the polar summer mesopause. Karlsson et al. (2009) found such a correlation using the extended CMAM, with stronger planetary wave activity producing a warmer winter stratosphere, followed 15-20 days later by a warmer summer polar mesopause. It seems plausible that the Q2DW may play a role in this inter-hemispheric coupling.

References

Karlsson, B., et al., 2009. Inter-hemispheric mesospheric coupling in a comprehensive middle atmosphere model. J. Atmos. Sol.-Terr. Phys., 71, 518–530.

Lieberman, R.S., 1999. Eliassen-palm fluxes of the 2-day wave. J. Atmos. Sci., 56, 2846–2861.

Limpasuvan, V., et al., 2005. The two-day wave in EOS MLS temperature and wind measurements during 2004-2005 winter. Geophys. Res. Lett., 32 (L17809).

Lübken, F.-J., et al., 2009. Stratospheric and solar cycle effects on long-term variability of mesospheric ice clouds. J. Geophys. Res., 144 (D00I06).

McCormack, J. P., et al., 2009. Evolution of the quasi-2-day wave during January 2006. J. Geophys. Res., 114 (D20115).

McLandress, C., et al., 2006. Large-scale dynamics of the mesosphere and lower thermosphere: An analysis using the extended CMAM. J. Geophys. Res., 111 (D17111).

Pendlebury, D., 2011. A simulation of the quasi 2-day wave and its effect on variability of the summertime mesopause temperature, J. Atmos. Sol.-Terr. Phys., submitted.

Stockwell, R. G., et al., 1996. Localization of the complex spectrum: The S transform. IEEE Transactions on Signal Processing, 44, 998–1001.

Acknowledgements

Thanks to Mike Neish and Stephen Beagley for help with the CMAM data. Thanks to Andreas Jonsson, Charles McLandress and Ted Shepherd for useful scientific discussion. This research was supported by the Canadian Foundation for Climate and Atmospheric Sciences and the Canadian Space Agency through the C-SPARC Network.